The Journal of Engineering

The 14th IET International Conference on AC and DC Power Transmission (ACDC 2018)

IET Journals
The Institution of Engineering and Technology

eISSN 2051-3305
Received on 4th September 2018
Accepted on 19th September 2018
E-First on 6th February 2019
doi: 10.1049/joe.2018.8880
www.ietdl.org

Analysis of the influence of dynamic components of AC/DC system on transient voltage stability based on energy function method

Wenqian Zhang[1] ✉, *Zhaobin Du*[1], *Changshu Huang*[1], *Chengjun Xia*[1], *Yao Zhang*[1]

[1]*College of Electric Engineering, South China University of Technology, Guangzhou, People's Republic of China*

✉ *E-mail: 907128867@qq.com*

Abstract: With the interconnection of large power networks, transient voltage stability of AC/DC power systems has been paid more attention in recent years. To investigate main influence of generating facility, high-voltage direct current (HVDC) and motor load for transient voltage stability, from the perspective of the generalised branch potential energy, the new indexes, and analysis method is proposed here. First, an energy function for AC/DC system is constructed with major dynamic components, namely classical HVDC control systems and motors in third-order model. Accordingly, the influence effects of the above major dynamic elements are investigated based on indexes from the corresponding generalised branch potential energy. With the rule of change in transient potential energy distribution in the network and information in stability margins, an evaluating procedure is established. Here, the judgment of transient voltage stability employs a heuristic energy function method. Finally, simulation tests on three-machine system with a HVDC transmission line are conducted in PSAT package, and the obtained results demonstrate the feasibility and effectiveness of the proposed method.

1 Introduction

Under the background of the power transmission from west to east in China, the electric network has become more and more complex with many HVDC transmission lines in use [1, 2]. The resulting large-scale grid poses many challenges in system operation safety, one of which is the transient voltage stability problem. The research of transient voltage stability could be reviewed two decades ago [3, 4]. The judgement of transient voltage instability from other instability phenomena could be made based on some methods [4, 5]. However, with more HVDC subsystems added into current dynamic components, such as generators and motors, many research topics of transient voltage stability of AC/DC system are still worth exploring [6, 7]. Especially at the receiving end of AC/DC system, several HVDC lines locate closely and by which usually a lot motor loads are supplied. In these situations, if the transient voltage instability problem exists, power engineers are interested in the influence of different kinds of dynamic components on such a problem.

The influence of dynamic components on system transient stability may be analysed by time-domain simulation method [7] with parameters setting change. However, it is not easy to find some measures telling the difference among components. Since energy function method can be used to analyse the power system stability and provide stability margin information, it becomes an important method [8–10] as well as time-domain simulation. Although energy function method arises from simple system model, many efforts have been put into introducing more dynamic models, like high-order motors [11] and HVDC systems [9, 10]. In fact, the energy function method has been tried to apply for the transient voltage stability analysis [8, 12, 13]. Based on the energy function method and some heuristic techniques, the voltage problem caused by motor instability is addressed [5]. Nevertheless, thyristor-controlled type HVDC, requiring more reactive power than normal in recovery after faults [1, 11], makes the situation confused compared to the reported case with motors only. It needs more methods since related works on this topic report less.

Here, a new analysis method is studied. The transient voltage stability is first judged with system bifurcation conditions and heuristic technique as possible. After that, based on local energy function method [14, 15] and its application on generalised branch potential energies [16–18], the exciter, HVDC, and load are modelled as the generalised branch, and the potential energies of different branches, after formatted according to the power scale, will be compared. The final evaluation on influence effect of dynamic components could be obtained with the above indexes relating the potential energy, as a uniform measure.

The system model with major dynamic components is presented in Section 2, and the energy function for these models is constructed in Section 3, after that a preliminary analysis method on influence of dynamic components on transient voltage stability is discussed. Simulation tests on a sample system are conducted to show the effect of the proposed method before the conclusion is drawn.

2 System modelling

Fourth-order generator model is used here and its mathematical equations [10] as below,

$$\begin{aligned}
\frac{\mathrm{d}\delta_i}{\mathrm{d}t} &= \omega_i \\
M_i\frac{\mathrm{d}\omega_i}{\mathrm{d}t} &= P_{\mathrm{mi}} - P_{\mathrm{ei}} - D_t\omega_i \\
T'_{\mathrm{doi}}\frac{\mathrm{d}E'_{\mathrm{qi}}}{\mathrm{d}t} &= E_{\mathrm{fdi}} - \frac{X_{\mathrm{di}}}{X'_{\mathrm{di}}}E'_{\mathrm{qi}} + \frac{X_{\mathrm{di}} - X'_{\mathrm{di}}}{X'_{\mathrm{di}}}V_i\cos(\delta_i - \theta_i) \\
T_{\mathrm{vi}}\frac{\mathrm{d}E_{\mathrm{fdi}}}{\mathrm{d}t} &= -E_{\mathrm{fdi}} - \mu_i k_i V_i\cos(\delta_i - \theta_i) + \mathrm{l}_i
\end{aligned} \tag{1}$$

where δ_i represents the rotor angle of the generator i, while ω_i represents the velocity of the generator. P_{mi} represents the generator mechanical power and P_{ei} is the generator electromagnetic power. T'_{doi} represents the d-axis transient time constant. E'_{qi} represents the q-axis transient potential. E_{fdi} represents excitation potential.

The HVDC system, which includes the controllers of the rectifier and inverter and the rule of voltage control, current control and constant extinction angle control, as below,

$$\begin{cases} \dfrac{\mathrm{d}X_1}{\mathrm{d}t} = \dfrac{1}{T_{c3}}(I_d - X_1) \\ \dfrac{\mathrm{d}\alpha_2}{\mathrm{d}t} = \dfrac{K_{c2}}{T_{c2}}(I_{\mathrm{dref}} - X_1) \\ \alpha_R = \begin{cases} \alpha_{\mathrm{Rmax}}, & \alpha_R \geq \alpha_{\mathrm{Rmax}} \\ K_{c1}(I_{\mathrm{dref}} - X_1) + \alpha_2, & \alpha_{\mathrm{Rmin}} \leq \alpha_R \leq \alpha_{\mathrm{Rmax}} \\ \alpha_{\mathrm{Rmin}}, & \alpha_R \leq \alpha_{\mathrm{Rmin}} \end{cases} \end{cases} \tag{2}$$

$$\begin{cases} I_{\mathrm{drefmax}}, & V_{\mathrm{dR}} \geq V_{\mathrm{dRmax}} \\ K_0(V_{\mathrm{dR}} - V_{\mathrm{dR0}}), & V_{\mathrm{dRmin}} \leq V_{\mathrm{dR}} \leq V_{\mathrm{dRmax}} \\ I_{\mathrm{drefmin}}, & V_{\mathrm{dR}} \leq V_{\mathrm{dRmin}} \end{cases} \tag{3}$$

$$\begin{cases} \dfrac{\mathrm{d}X_2}{\mathrm{d}t} = \dfrac{1}{T_{V3}}(V_{dI} - X_2) \\ \dfrac{\mathrm{d}\beta_2}{\mathrm{d}t} = \dfrac{K_{V2}}{T_{V2}}(V_{\mathrm{dref}} - X_2) \\ \beta = \begin{cases} \beta_{\max}, & \beta \geq \beta_{\max} \\ K_{V1}(V_{\mathrm{dref}} - X_2) + \beta_2, & \beta_1 \leq \beta \leq \beta_{\max} \end{cases} \end{cases} \tag{4}$$

$$\frac{\mathrm{d}\beta}{\mathrm{d}t} = -\frac{K_{V1}}{T_{V3}}V_{\mathrm{dI}} + \frac{K_{V2}}{T_{V2}}V_{\mathrm{dref}} + \left(\frac{K_{V1}}{T_{V3}} - \frac{K_{V2}}{T_{V2}}\right)X_2 \tag{5}$$

$$\begin{cases} \dfrac{\mathrm{d}X_3}{\mathrm{d}t} = \dfrac{1}{T_{\mu 3}}(\gamma - X_3) \\ \dfrac{\mathrm{d}\beta_3}{\mathrm{d}t} = \dfrac{K_{\mu 2}}{T_{\mu 2}}(\gamma_{\mathrm{ref}} - X_3) \\ \beta = \begin{cases} K_{\mu 1}(\gamma_{\mathrm{ref}} - X_3) + \beta_3, & \beta_{\min} \leq \beta \leq \beta_1 \\ \beta_{\min}, & \beta \leq \beta_{\min} \end{cases} \end{cases} \tag{6}$$

$$\frac{\mathrm{d}\beta}{\mathrm{d}t} = -\frac{K_{\mu 1}}{T_{\mu 3}}\gamma + \frac{K_{\mu 2}}{T_{\mu 2}}\gamma_{\mathrm{ref}} + \left(\frac{K_{\mu 1}}{T_{\mu 3}} - \frac{K_{\mu 2}}{T_{\mu 2}}\right)X_3 \tag{7}$$

The detailed parameters can be seen in [7, 10, 12].

The third-order model of motor load is shown as below,

$$\begin{cases} \dfrac{T'_{L\mathrm{doi}}}{X_i - X'_i}\dfrac{\mathrm{d}E'_{\mathrm{Li}}}{\mathrm{d}t} = -\dfrac{X_i}{X_i - X'_i}E'_{\mathrm{Li}} + \dfrac{V_i\cos(\delta_{\mathrm{Li}} - \theta_i)}{X'_i} \\ \dfrac{\mathrm{d}\delta_{\mathrm{Li}}}{\mathrm{d}t} = -s_i + \dfrac{X_i - X'_i}{T'_{L\mathrm{doi}}E'_{\mathrm{Li}}} \cdot \dfrac{V_i\sin(\delta_{\mathrm{Li}} - \theta_i)}{X'_i} \\ M_{\mathrm{Li}}\dfrac{\mathrm{d}s_i}{\mathrm{d}t} = T_{\mathrm{mi}} - T_{\mathrm{ei}} = T_{\mathrm{mi}} - \dfrac{E'_{Li}V_i\sin(\delta_{\mathrm{Li}} - \theta_i)}{X'_i} \end{cases} \tag{8}$$

$$i = n+2, n+3, \ldots, n+N+1;$$

where $T'_{L\mathrm{doi}}$ represents the stator open time constant. M_{Li} represents the inertia time constant. E'_{Li} represents the internal potential amplitude and δ_{Li} represents the internal potential angle.

3 Derivation of the energy function

The following energy functions are obtained by the first integral method. The derivation of them is omitted here as space is limited.

3.1 Energy function of the generator

$$U_k = \sum_{i=1}^{n}\frac{1}{2}M_i\omega_i^2 \tag{9}$$

(9) is the kinetic energy, and the following expressions are all potential energies backward.

$$\begin{aligned} U_g = & -\sum_{i=1}^{n}P_{\mathrm{mi}}\delta_i - \sum_{i=1}^{n}\frac{V_iE'_{\mathrm{qi}}\cos(\delta_i - \theta_i)}{X_i} \\ & + \sum_{i=1}^{n}\frac{\left(X'_{\mathrm{di}} + X_{\mathrm{qi}}\right) - \left(X'_{\mathrm{di}} - X_{\mathrm{qi}}\right)\cos 2(\delta_i - \theta_i)}{4X_{\mathrm{qi}}X'_{\mathrm{di}}}V_i^2 \\ & + \sum_{i=1}^{n}\frac{X_{\mathrm{di}}}{2X'_{\mathrm{di}}(X_{\mathrm{di}} - X'_{\mathrm{di}})}E'^2_{\mathrm{qi}} - \frac{1}{2}\boldsymbol{E}^{\mathbf{T}}\boldsymbol{B}^{-1}\boldsymbol{A}\boldsymbol{E} - (\boldsymbol{B}^{-1}\boldsymbol{C})^{\mathbf{T}} \end{aligned} \tag{10}$$

where $E = [E_1, \ldots, E_n]^{\mathrm{T}}$, $E_i = \left[E'_{\mathrm{qi}}E_{\mathrm{fdi}}\right]$,

$$\boldsymbol{T} = \mathrm{blockdiag}[T_1, \ldots, T_n],\ \boldsymbol{T_i} = \begin{bmatrix} T'_{\mathrm{doi}} & 0 \\ 0 & T_{\mathrm{vi}} \end{bmatrix},$$

$$\boldsymbol{A} = \mathrm{blockdiag}[A_1, \ldots, A_n],\ \boldsymbol{A_i} = \begin{bmatrix} 0 & 1 \\ -\dfrac{\mu_i k_i X'_{\mathrm{di}}}{X_{\mathrm{di}} - X'_{\mathrm{di}}} & -1 \end{bmatrix}$$

$$\boldsymbol{B} = \mathrm{blockdiag}[B_1, \ldots, B_n],\ \boldsymbol{B_i} = \begin{bmatrix} \dfrac{X_{\mathrm{di}} - X'_{\mathrm{di}}}{X'_{\mathrm{di}}} & -\rho_i \\ -\mu_i k_i & \rho_i \end{bmatrix}$$

$\boldsymbol{C} = [C_1, \ldots, C_n]^{\mathrm{T}}$, $\boldsymbol{C_i} = [0 \quad l]$, where ρ_i is the parameter to make $B_i^{-1}T_i$ positive definite. For any non-zero matrix vector, $x^{\mathrm{T}}B_i^{-1}T_ix > 0$ holds [10]. $i = 1, 2, \ldots, n$.

3.2 Energy function of the HVDC system

$$U_R = -V_R\sum_{j=1}^{n+N+1}V_jB_{\mathrm{Rj}}\cos(\theta_R - \theta_j) - \frac{1}{2}V_R^2B_{\mathrm{RR}} \tag{11}$$

$$U_I = -V_I\sum_{j=1}^{n+N+1}V_jB_{\mathrm{Ij}}\cos(\theta_I - \theta_j) - \frac{1}{2}V_I^2B_{II} \tag{12}$$

$$U_d = \int P_{\mathrm{dR}}\mathrm{d}\theta_R + \int\frac{Q_{\mathrm{dR}}}{V_R}\mathrm{d}V_R + \int P_{\mathrm{dI}}\mathrm{d}\theta_I + \int\frac{Q_{\mathrm{dI}}}{V_I}\mathrm{d}V_I \tag{13}$$

$$U_{\mathrm{DC}} = -V_RV_IB_{\mathrm{IR}}\cos(\theta_I - \theta_R) \tag{14}$$

where U_R represents the rectifier side node potential energy function. U_I represents the inverted side node's potential energy function. U_d represents the potential energy function that generated by transmitting power through the HVDC transmission line. U_{DC} represents the HVDC network potential energy function.

3.3 Energy function of the load

$$U_{L1i} = -\sum_{i=n+2}^{n+N+1}\int P_{L1i}\mathrm{d}\theta_i - \sum_{i=n+2}^{n+N+1}\int\frac{Q_{L1i}(V_i)}{V_i}\mathrm{d}V_i \tag{15}$$

$$\begin{aligned} U_{L2i} = & \sum_{i=n+2}^{n+N+1}\frac{1}{2}M_{Li}s_i^2 - \sum_{i=n+2}^{n+N+1}\int M_{\mathrm{Li}}\frac{X_i - X'_i}{T'_{L\mathrm{doi}}E'_{\mathrm{Li}}} \times I_{\mathrm{qi}}\mathrm{d}s_i \\ & + \sum_{i=n+2}^{n+N+1}T_{\mathrm{mi}}\delta_{\mathrm{Li}} - \sum_{i=n+2}^{n+N+1}\frac{X'_iI_{\mathrm{xi}}^2 + X'_iI_{\mathrm{yi}}^2}{2} \\ & + \sum_{i=n+2}^{n+N+1}\frac{1}{2(X_i - X'_i)}E'^2_{\mathrm{Li}} \end{aligned} \tag{16}$$

where U_{L1i} and U_{L2i} represent the static load potential energy function and dynamic load (motor) potential energy function, respectively.

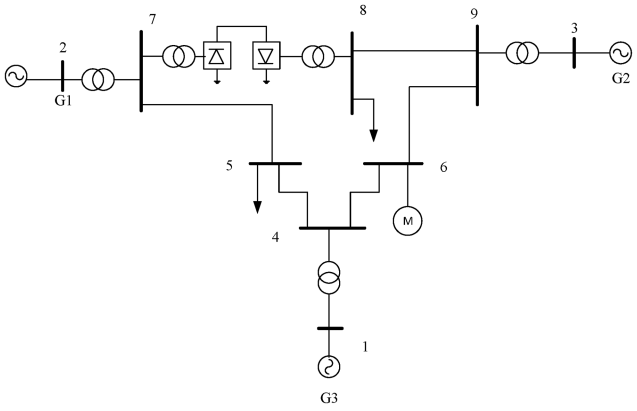

Fig. 1 *Three-machine nine-bus system with a HVDC*

3.4 Energy function of the AC network

$$U_{\mathrm{AC}} = -\sum_{i=1}^{n+1}\sum_{j=n+2}^{n+N+1} V_i V_j B_{\mathrm{Rj}} \cos(\theta_R - \theta_j) - \sum_{n+1<i<j}^{n+N+1} V_i V_j B_{\mathrm{ij}} \cos(\theta_i - \theta_j) - \sum_{1\le i<j}^{n+1} V_i V_j B_{\mathrm{ij}} \cos(\theta_i - \theta_j) - \sum_{i=1}^{n+N+1} \frac{1}{2} V_{\mathrm{ii}}^2 B_{\mathrm{ii}}$$

4 Evaluation method

The excessive concentration of transient energy of post-fault system is the main cause of system angle instability, and the generator kinetic energy changes will be reflected in the various local potential changes according to the parameters and characteristics of various components of the system [14]. Inspired by the above idea and with the skill of transient voltage analysis, this paper presents a new evaluation method on the influence of different system dynamic components on transient voltage stability. The key procedure of the method is as follows:

Step 1: The transient voltage stability is first judged with system bifurcation conditions and heuristic technique as possible, as shown in [4, 8, 12, 13].

Step 2: Based on local energy function method and its application on generalised branch potential energies (13), (15) or (16) are used for the generalised branches potential energies of HVDC and load, respectively.

Step 3: When there are more than one branches of the same kind, like 2 or 3 HVDC links in a system, the corresponding branch class is formatted according to the power scale and then the influence effects are compared with each other, like first HVDC potential versus second HVDC potential.

Step 4: The maximum incremental of potential energy of the generalised branches are calculated and marked by the $\Delta U_{\mathrm{Max},k}$ for the system swing when the peak of potential energy occurs, where k is the kth generalised branch and incremental means the peak subtracts the valley at the same swing. Here, $\Delta U_{\mathrm{Max},k}$ is preliminarily defined as the evaluating indexes, the function of $\Delta U_{\mathrm{Max},k}$ and reactive power consumed by dynamic components will be studied in future. With the heuristic rule of change in transient potential energy distribution in the whole network, the larger the absolute value of the above index is, the more significant the corresponding dynamic component for transient voltage stability is. Thus, the final result on the influence of different components could be achieved.

5 Simulations

The tests of the proposed method are on the PSAT package. The three-machine nine-bus system interconnected with the HVDC is used as the simulation system, which is shown in Fig. 1. The parameters about the system can refer to the literature [12]. Three-phase line-to-ground fault is set on the bus 5 at 1 s. The maximum lasting time of fault for critical transient voltage stability is about 230 ms.

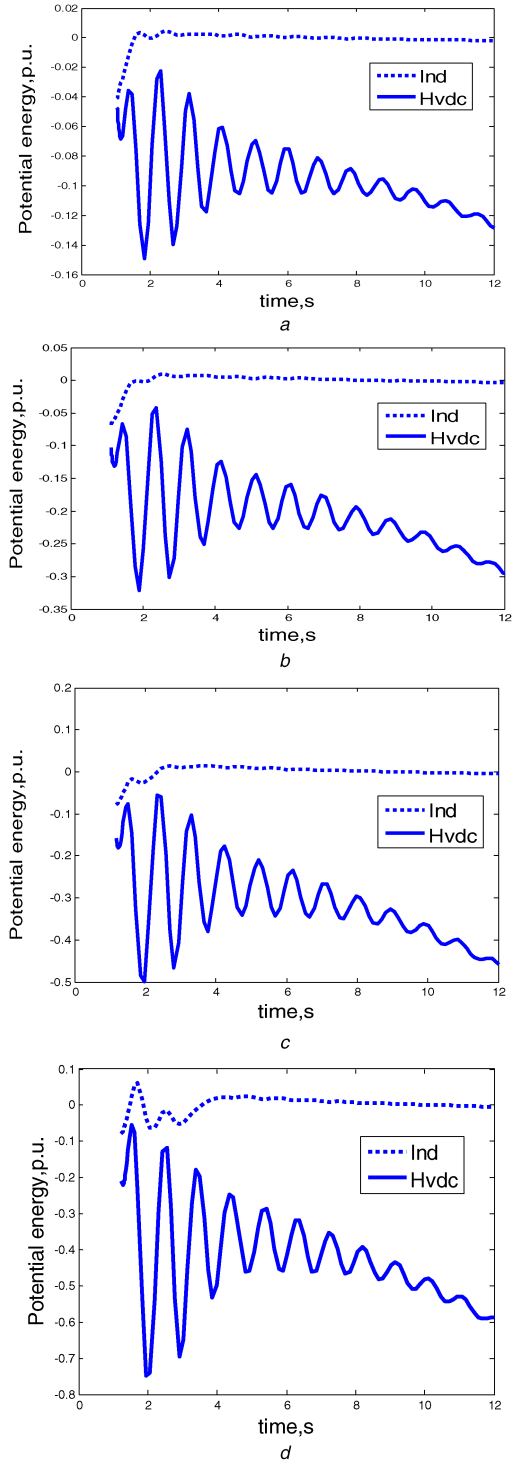

Fig. 2 *Induction motor load, HVDC potential energy*
(a) Clear time is 1.05 s, ***(b)*** Clear time is 1.11s, ***(c)*** Clear time is 1.17 s, ***(d)*** Clear time is 1.23s

The cases for critical stability and instability are simulated and the resulting generalised branches potential energies are checked below.

As the likely singularity occurs in PSAT simulation when the clear time is at 1.24 s, which results the calculation termination. Thus, the potential curves corresponding to HVDC and induction motor load are simulated at the clear time 1.05 s, 1.11 s, 1.17, and 1.23 s, respectively, which are show in Fig. 2*a–d*. Where dotted line and solid line represent the potential energy of induction motor load and HVDC system, respectively.

Table 1 Potential of each dynamic components in the first swing

Clear time	1.23 s	1.17 s	1.11 s	1.05 s
HVDC	0.69551	0.42322	0.25497	0.11354
motor	0.12285	0.00827	0.0010056	0.0010056

Table 2 Change of the voltage value before and after fault

	Before	After	$\triangle v$
HVDC	0.98	0.8678	0.1122
motor	1.0114	0.873	0.1384

From Table 1, the authors can see, HVDC will suffer more of the potential energy converted by the generator's kinetic energy in the first swing. Meanwhile, with the increase of fault duration, the change of potential energy of induction motor in the first pendulum gradually increases from less. Therefore, one may see that the main weak potential of the local potential occurs at the receiving-end HVDC, and the second local potential weak point is at induction motor load.

The change of voltage value before and after fault corresponding to receiving-end HVDC (bus8) and induction motor load (bus6) are compared prior to the critical clear time, which are shown in Table 2. From the table, the authors can see, in the case of the system remains stable after fault, the voltage drop of the induction motor load is larger than the receiving-end HVDC, which is shown in Figs. 3 and 4.

From the time domain simulation results prior to the voltage instability, when the power angle of the three generators has not yet been split, the terminal voltage of the receiving-end HVDC and the induction motor have already dropped to 0.8 and with a trend downward, which considered as voltage instability. At the same time, comparing the slip curve of induction motor between stability and instability cases after fault (shown in Fig. 5), the authors can see that there is a tendency that the slip of induction motor monotonically increase and motor stalls.

In summary, from Table 1, Table 2 and the time-domain simulation results of instability, it may be seen that the induced load is the main weak local component of the system and the HVDC system is probably a fragile part under transient voltage instability. However, this example is relatively simple and the electrical distance between the HVDC system and the induction motor load is short, the interaction between them and the independence effect of the HVDC system has yet to be further analysed in more complicated cases.

6 Conclusion

Here, an evaluation method on the influence of different system dynamic components on transient voltage stability of AC/DC system is studied. Based on the judgment of transient voltage stability with bifurcation condition and heuristic information, an evaluation index is preliminarily provided, which is derived from potential energy of generalised branches corresponding to HVDC and load, respectively. This idea is tested in PSAT package, and the obtained results demonstrate the feasibility and effectiveness of the propose method. The future work includes the relation between the bifurcation condition and the generalised branch potential expression etc.

7 Acknowledgments

The paper is sponsored by the National Natural Science Foundation of China (51577071) and Guangdong Natural Science Foundation (2015A030313202).

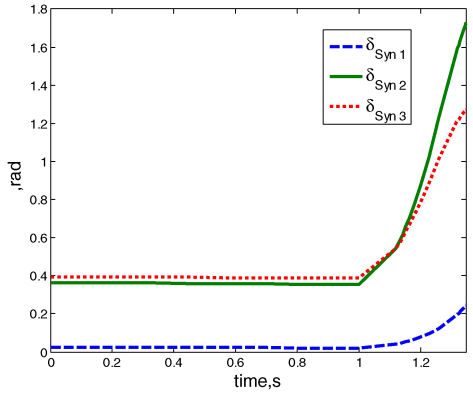

Fig. 3 *Generator power angle*

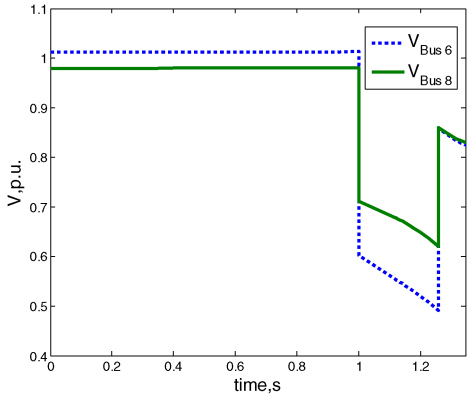

Fig. 4 *Voltage of the receiving-end HVDC and the Motor*

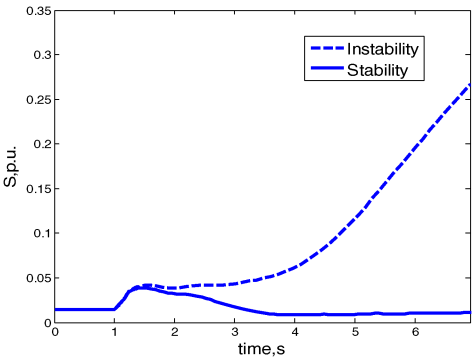

Fig. 5 *Slips of the motor in the case of stable and unstable*

8 References

[1] Shao, Y., Tang, Y., Guo, X.J., *et al.*: 'Analysis on commutation failures in multi-infeed HVDC transmission systems in north China and east China power grids planned for UHV power grids in 2015', *Power Syst. Technol.*, 2011, **35**, (10), pp. 9–15

[2] Li, Y., Luo, Y., Xu, S.K., *et al.*: 'VSC-HVDC transmission technology: application, advancement and expectation', *China South. Power Grid Technol.*, 2015, **9**, (1), pp. 7–13

[3] Wang, J.J., Zhang, Y., Xia, C.J., *et al.*: 'Survey of studies on transient voltage stability of AC/DC power system', *Power Syst. Technol.*, 2008, **32**, (12), pp. 30–34

[4] Zhong, W.Z.: '*Mechanism research of transient voltage stability in receiving-end grid*' (China Electric Power Science Research Institute, Beijing, 2008)

[5] Lin, S.J., Liu, M.B.: 'Computation of controlling unstable equilibrium point corresponding to the instability mode of transient voltage', *J. South China Univ. Technol. (Nat. Sci. Ed.)*, 2009, **37**, (11), pp. 88–94

[6] Lin, Y.Z., Cai, Z.X.: 'Transient stability analysis of AC/DC power system based on PEBS method', *Electr. Power Autom. Equip.*, 2009, **29**, (1), pp. 24–28

[7] Ni, Y.X., Chen, S.C., Zhang, B.L.: '*Theory and analysis of dynamic power systems*' (Tsinghua University Press, Beijing, 2005, May 1st. 2002)

[8] Praprost, K.L., Loparo, K.A.: 'An energy function method for determining voltage collapse during a power system transient', *IEEE Trans. Circuits Syst. I, Fundam. Theory Appl.*, 1994, **41**, (10), pp. 635–651

[9] Fernandopulle, N., Alden, R.T.H.: 'Incorporation of detailed HVDC dynamics into transient energy functions', *IEEE Trans. Power Syst.*, 2005, **20**, (2), pp. 1043–1052

[10] Jiang, N., Chang, H.D.: 'Energy function for power system with detailed DC model: construction and analysis', *IEEE Trans. Power Syst.*, 2013, **28**, (4), pp. 3756–3764
[11] Min, Y., Chen, L.: 'Energy function of power system incorporating the induction model', *Sci. China (Ser. E: Technol. Sci.)*, 2007, **37**, (9), pp. 1117–1125
[12] Zhan, F.J., Du, Z.B., Zhao, F.*, et al.*: 'Analysis of the transient voltage stability of AC/DC system based on numerical energy function method'. 2016 IEEE PES Asia-Pacific Power and Energy Engineering Conf. (APPEEC), Xi'an, 2016, pp. 2204–2208
[13] Zhan, F.J., Du, Z.B., Huang, B.X.*, et al.*: 'Study of transient voltage stability of power system based on heuristic energy function method'. 2016 Int. Conf. on Smart Grid and Clean Energy Technologies (ICSGCE), Chengdu, China, 2016, pp. 354–358
[14] Cai, G.W., Mu, G., Chan, K.W.*, et al.*: 'Branch potential energy method for power system transient stability assessment based on network dynamic variables', *Proc. CSEE*, 2004, **24**, (5), pp. 1–6
[15] Yuan, W.P., Li, L., Chen, J.R.*, et al.*: 'Transient stability evaluation of power system based on line potential energy method', *Guangdong Electr. Power*, 2008, **21**, (1), pp. 1–6
[16] Yun, L., Liu, D.C., Liao, Q.F.*, et al.*: 'Power exchange capacity among UHV power grids base on branch transient energy', *Electr. Power Autom. Equip.*, 2012, **32**, (3), pp. 7–12
[17] Li, Y., Liu, J.Y., Li, X.Y.*, et al.*: 'Assessment of vulnerable vines in power grid based on entropy of generalized branch energy', *Proc. CSEE*, 2013, **33**, (34), pp. 187–196
[18] Meng, X.X., Liu, M.G., Zhang, Q.Z.*, et al.*: 'Mechanism analysis of transient potential energy distribution based on network structure', *Autom. Electr. Power Syst.*, 2016, **40**, (13), pp. 41–47